DMD Fast Forward. Published on March 29, 2011 as doi:10.1124/dmd.111.038075

Use of transporter knockdown Caco-2 cells to investigate the *in vitro* efflux of statin drugs[†]

Jibin Li, Donna A. Volpe*, Ying Wang, Wei Zhang, Chris Bode, Albert Owen, and Ismael J. Hidalgo

Absorption Systems L.P., Exton, PA (JL, WZ, YW, CB, AO, IH) and

The Food and Drug Administration, Division of Drug Safety Research, Silver Spring, MD (DV)

DMD Fast Forward. Published on March 29, 2011 as DOI: 10.1124/dmd.111.038075
This article has not been copyedited and formatted. The final version may differ from this version.
DMD #38075

Running Title: Efflux of Statin Drugs in Knockdown Caco-2 Cells

Corresponding Author: Ismael J. Hidalgo, Ph.D., Absorption Systems LP, 436 Creamery Way, Suite 600, Ex ton, PA 19341–2556, Phone: (610) 280 7300, F ax: (610) 280-9667, Email: ihidalgo@absorption.com

Text pages: 27

Tables: 2

Figures: 6

References: 33

Word count

Abstract: 245

Introduction: 574

Discussion: 1,455

Non-standard abbreviations: A, apical; B, basolateral; ABC, ATP-binding cassette; P-gp, P-glycoprotein; BCRP, breast cancer resistance protein; MRP2, multidrug resistance associated protein 2; KD, knockdown; VC, vector control; P_{app}, apparent permeability; BSP, bromosulfophthalein; E3S, estrone-3-sulfate; FTC, fumitremorgin; HBSS, Hanks' balanced salts solution; TEER, transepithelial electrical resistance; qPCR, quantitative polymerase chain reaction; LC-MS/MS, liquid chromatography with triple quadruple tandem mass spectrometry; SNP, single nucleotide polymorphism; shRNA, small hairpin RNA; siRNA, small interfering RNA.

DMD Fast Forward. Published on March 29, 2011 as DOI: 10.1124/dmd.111.038075
This article has not been copyedited and formatted. The final version may differ from this version.

ABSTRACT:

The objective of the present study was to determine the efflux transporters responsible for acid and lactone statin drugs efflux using transporter knockdown Caco-2 cells. The bidirectional transport was determined in Caco-2 cell monolayers in which the expression of either P-glycoprotein (P-gp), breast cancer resistance protein (BCRP) or multidrug resistance associated protein 2 (MRP2) was knocked down by transduction with lentivirus containing human transporter targeted shRNAs. Cells transduced with lentivirus containing non-targeted shRNA served as vector control. Atorvastatin, lovastatin and rosuvastatin displayed extremely low apical-to-basolateral (A-B) transport, which made the $P_{app,A-B}$ values too unreliable to calculate the efflux ratio. Thus, transport comparisons were performed using the B-A permeability ($P_{app,B-A}$) values. Presented in the order of vector control, P-gp, BCRP, and MRP2 knockdown Caco-2 cells, the $P_{app,B-A}$ values ($\times 10^{-6}$, cm/s) were 28.1±1.3, 8.6±2.9, 20.3±1.8 and 21.5±1.6 for atorvastatin; 96.1±7.1, 25.3±3.5, 57.3±9.8 and 48.2±2.3 for fluvastatin; 14.1±1.9, 4.6±1.7, 5.8±0.7 and 6.6±1.8 for rosuvastatin, respectively. Lovastatin and simvastatin showed no efflux in the vector control or knockdown cell monolayers in either lactone or acid forms. Results indicate that atorvastatin, fluvastatin and rosuvastatin were transported by P-gp, BCRP, and MRP2. On the other hand, neither the lactone nor the resulting acid of lovastatin and simvastatin were transported by P-gp, BCRP or MRP2. The current study demonstrated that the transporter knockdown Caco-2 cells are useful tools for studying drug-transporter interactions and should help eliminate some of the ambiguity associated with the identification of drug-transporter interactions based on chemical inhibitors alone.

DMD Fast Forward. Published on March 29, 2011 as DOI: 10.1124/dmd.111.038075
This article has not been copyedited and formatted. The final version may differ from this version.

Introduction

Statins lower low-density lipoprotein cholesterol levels by competitively inhibiting 3-hydroxy-3-methylglutaryl coenzyme A (HMG-CoA) reductase activity, the rate-limiting step in cholesterol synthesis. They are among the most widely used drugs worldwide for the treatment and prevention of ischaemic heart disease. Most statins are administered in the orally active β-hydroxy acid form, the exceptions being lovastatin and simvastatin, which are given as inactive lactone prodrugs. After oral administration, the fractional absorption of statin drugs ranges from 30% to >98%, and the bioavailability ranges from <5% to 60% (Neuvonen et al., 2006). Statin drugs are eliminated primarily through the hepatobiliary route and renal excretion constitutes a minor route of elimination, except for pravastatin. Although generally well tolerated, statin drugs can cause side effects such as myopathy, whose symptoms range from benign myalgias to life-threatening rhabdomyolysis (Neuvonen et al., 2006). In addition, the side effects of statin drugs are frequently associated with drug-drug interactions resulting from their chronic administration to patients who are likely to be taking multiple drugs.

Previous statin transport studies have suggested that cellular uptake and excretion of these drugs is mediated by a variety of membrane transporters. Atorvastatin, lovastatin, and simvastatin have been reported to be effluxed by P-glycoprotein (P-gp) (Hochman et al., 2004; Chen et al., 2007; Kitamura et al., 2008), whereas the involvement of P-gp on the efflux of rosuvastatin is controversial (Huang et al., 2006; Kitamura et al., 2008). In contrast to ATP-binding cassette (ABC) efflux transporters, which differ in their affinity for and functional transport of various statins, the exchange transporters from the solute carrier (SLC) family organic anion transporting protein (OATP) 1B1 was reported to mediate the cellular uptake of all statin drugs except fluvastatin (Kitamura et al., 2008; Ieiri et al., 2009).

The purpose of this study was to identify the role of the most important intestinal ABC efflux transporters, P-gp, breast cancer resistance protein (BCRP), or multidrug resistance

protein 2 (MRP2), in the intestinal efflux of statin drugs through the use of knockdown (KD) Caco-2 cell clones in which the expression of P-gp, BCRP or MRP2 were silenced with lentiviral vectors containing shRNA targeted to unique mRNA sequences in each efflux transporter (Zhang et al., 2009). Human intestinal cell lines such as Caco-2 are widely used to study drug absorption and efflux pathways in vitro (Hidalgo, 2001; Elsby et al., 2008). By evaluating the bidirectional permeability of acid or lactone statins in the KD cells we determined the role of various transporters on statin transport. In addition, the system permitted observation of a general distinction between acid and lactone statins in terms of their interaction with P-gp. Rosuvastatin was determined to be a substrate of various efflux transporters and additional experiments with chemical inhibitors provided complementary evidence for the involvement of P-gp, BCRP and MRP2 on rosuvastatin transport. We have shown that KD cell lines derived from Caco-2 cells constitute a valuable system for evaluating statin transport pathways. This system avoids the need to rely only on chemical inhibitors, which lack selectivity (Watanabe et al., 2005; Wang et al., 2008), to identify transporter-mediated drug-drug interactions. It also allows investigation of efflux mechanisms that may be extremely difficult to unravel using either non-cell based models such as membrane vesicles or animal cell lines transfected with human transporters; as compared to the Caco-2 model, these systems are less representative of the physiological factors found in human intestine (Polli et al., 2001; Elsby et al., 2008; Kitamura et al., 2008).

DMD Fast Forward. Published on March 29, 2011 as DOI: 10.1124/dmd.111.038075
This article has not been copyedited and formatted. The final version may differ from this version.

Materials and Methods

Chemicals. Atorvastatin calcium, fluvastatin sodium, lovastatin, rosuvastatin calcium and simvastatin were obtained from Toronto Research Chemicals (North York, Ontario, Canada). Digoxin, verapamil, bromosulfophthalein (BSP), estrone-3-sulfate (E3S), MK571 sodium salt, fumitremorgin C (FTC), propranolol HCl and atenolol were purchased from Sigma Aldrich (St. Louis, MO). Fetal bovine serum (FBS) was obtained from Omega (Tarzana, CA). Penicillin-streptomycin, non-essential amino acids (NEAA), L-glutamine, trypsin, and puromycin were obtained from Cellgro (Manassas, VA). Lucifer yellow, Hanks' balanced salts solution (HBSS), Dulbecco's modified Eagle's medium (DMEM), Dulbecco's phosphate buffered saline (DPBS), and N-[2-hydroxyethyl]piperazine-N'-[2-ethanesulfonic acid] (HEPES) were obtained from GIBCO/Invitrogen (Carlsbad, CA).

Transduction of Caco-2 cells with shRNAs. Parental Caco-2 cells were obtained from American Type Culture Collection (Manassas, VA, ATCC® Accession Number CRL-2102). The cells were maintained in DMEM with 4.5 g/L glucose, supplemented with 10% FBS, 1% NEAA, 2 mM L-glutamine, 100 U/mL penicillin, and 100 μg/mL streptomycin at 37°C in a humidified atmosphere of 5% CO_2 and 95% air. Lentivirus plasmid vectors containing shRNA inserts targeting human P-gp (Accession I.D. NM_000927), BCRP (Accession I.D. NM_004827), and MRP2 (Accession I.D. NM_000392) genes were obtained from Sigma (St. Louis, MO). The transduction procedure was described previously (Zhang et al., 2009). Briefly, the cells were plated in 96-well tissue culture plates at a density of 5×10^6 cell/well and transduced with 1 μg of P-gp-, BCRP-, or MRP2-targetting shRNA viral vector. Transduced cells were selected in culture medium containing 10 μg/mL puromycin. As transduction control, parental Caco-2 cells were also transduced with a lentivirus plasmid vector containing shRNA that does not match any known human genes (Sigma), and the transduction procedures were identical to those used with P-gp, BCRP, and MRP2 shRNA vectors. Transfected cells were maintained under

selection pressure of 10 μg/mL puromycin for at least 5 passages. After down-regulation of the efflux transporter of interest was verified by real-time PCR, the cells were seeded and grown on Transwell plate for transport experiment.

Cell Culture. Cells were seeded at 60,000 cells/cm^2 onto collagen-coated, microporous, polycarbonate membranes in 12-well Costar® Transwell® plates (1.13 cm^2 insert area, 0.4 μm pore size; Corning, NY). The culture medium was changed 24 h after seeding to remove cell debris and dead cells; afterwards the medium was changed every other day. The cells were maintained at 37°C in a humidified atmosphere of 5% CO_2 in air for three weeks to form confluent monolayers. The transport assay buffer was Hanks' balance salts solution containing 10 mM HEPES and 15 mM glucose at pH 7.4 (HBSSg buffer). Batches of cell monolayers were certified by measuring the transepithelial electrical resistance (TEER) values of the monolayers and the apparent permeability coefficient (P_{app}) of control compounds: Lucifer yellow (low permeability marker), atenolol (low permeability marker), propranolol (high permeability marker), and the efflux ratios of digoxin, E3S, and BSP (P-gp, BCRP, and MRP2 probe substrates, respectively). Lucifer yellow was assayed at 0.5 mM, and the other probes (atenolol, propranolol, digoxin, E3S and BSP) at 10 μM. The acceptance criteria for batches of cell monolayers usable in transport experiments were: TEER > 450 Ω×cm^2, Lucifer yellow $P_{app} < 0.4 \times 10^{-6}$ cm/s, atenolol $P_{app} < 0.5 \times 10^{-6}$ cm/s, propranolol P_{app} between 15×10^{-6} and 25×10^{-6} cm/s. Prior to the transport experiment, TEER values were measured for all cell monolayers, and only monolayers with TEER values that met the acceptance criteria were used in the study.

Efflux Transporter Gene Expression by Real-Time PCR. Total RNA was isolated from mature cell monolayers using RNeasy® Mini Kit (Qiagen®, Hilden, Germany) according to the manufacturer's protocol. Synthesis of cDNA was carried out from 1 μg of total RNA using QuantiTect® RT kit (Qiagen®, Hilden, Germany) for reverse transcription-polymerase chain

reaction (PCR) with random hexamer primers according to the manufacturer's protocol. Real-time quantitative PCR (qPCR) was performed using the LightCycler® 480 system (Roche Diagnostics, Mannheim, Germany). Primer and probes were designed using the Universal Probe Library (Roche, Basel, Switzerland). Each PCR reaction contained 10 ng cDNA, LightCycler® 480 probes master kit with 0.1 μM probe and 0.5 μM primers. The PCR reaction was run at 95°C for 10 min, followed by 45 amplification cycles of 95°C for 10 s, 60°C for 15 s, and 72°C for 1 s. Quantification of relative gene expression was performed using the $\Delta\Delta C_T$ method. The housekeeping gene β-actin was used for normalization. Fold change were calculated using vector control (VC) Caco-2 cells as the calibrator.

Western Blot Analysis for Efflux Transporter Proteins. Cells were lysed with ice-cold radioimmunoprecipitation assay lysis buffer (Santa Cruz Biotechnology, Inc. Santa Cruz, CA), and proteins were isolated following the manufacturer's protocol. Proteins (45 μg per lane) were separated on 4 to 20% SDS-polyacrylamide gel, then transferred to a PVDF membrane and blocked with 0.2% I-block solution in TBS containing 0.05% Tween 20. Blocked membranes were probed sequentially with antibodies against the proteins of interest: P-gp (C-219, Abcam, Cambridge, MA), BCRP (BXP-21), MRP2 and β-actin (Sigma-Aldrich). After washing, the membranes were reacted with the secondary antibodies. Protein-antibody complexes were visualized using SuperSignal West Femto Chemiluminescent Substrate (Pierce, Rockford, IL).

Statin Transport Assays. Five statin drugs (atorvastatin, fluvastatin, rosuvastatin, lovastatin and simvastatin) were selected for this study because they reflect a wide range of physicochemical properties (i.e. lipophilicity), chemical structures (acid and lactone), and interactions with transporters and/or metabolizing enzymes (Neuvonen et al., 2006). The transport assay included apical to basolateral (A-to-B) and basolateral to apical (B-to-A) transport rate

determinations for each statin in each cell line utilized in this study. The statin compound was prepared at 10 μM in HBSSg buffer containing the high and low permeability reference standards (10 μM atenolol and 10 μM propranolol, respectively). For A-to-B transport, 0.55 mL of compound-containing solution was dosed to the apical (donor) chamber and 1.5 mL of blank HBSSg buffer was applied to the basolateral (receiver) chamber. For B-to-A transport, 1.55 mL of compound-containing solution was dosed to the basolateral (donor) chamber and 0.5 mL of blank HBSSg was added to the apical (receiver) chamber. At 30, 60, 90, and 120 min, 0.2 mL samples were withdrawn from the receiver chambers. The sample volume removed from the receiver chambers was replaced with an equal volume of pre-warmed blank HBSSg buffer. At 0 and 120 min, 0.05 mL of samples were collected from the donor chambers. Upon collection, the samples were immediately combined with 0.2 mL of 100% acetonitrile and stored at 4°C until sample analysis. For rosuvastatin kinetic studies, B-to-A transport rates of rosuvastatin across Caco-2 cell monolayers were measured as a function of rosuvastatin concentration at 37°C and 4°C. For rosuvastatin inhibition studies, Caco-2 cell monolayers were pre-incubated with an inhibitor in both apical and basolateral chambers for 30 min, then bidirectional transport of rosuvastatin was conducted in the presence of the inhibitor in both chambers.

Sample Analyses. Concentrations of statin drugs were analyzed using reverse phase liquid chromatography with triple quadruple tandem mass spectrometry (LC-MS/MS) methods. Samples were diluted with acetonitrile:HBSS pH7.4 (50:50 v/v) as follows: receiver samples were diluted 4-fold; donor samples were diluted 20-fold. The HPLC equipment consisted of a Perkin-Elmer series 200 autosampler and a Perkin-Elmer series 200 micro pumps (Waltham, MA). Chromatography was performed at ambient temperature using a 50 mm × 2.0 mm i.d. 4 μm Phenomenex® Synergi™ Polar-RP analytical column (Torrance, CA). The mobile phase consisted of 0.2% formic acid (aqueous phase) and 90:10 ACN:MeOH (organic phase). Typical gradients

started at 10% aqueous phase, changed linearly to 95% organic phase over 3.0 min, held at 95% organic phase for 1.0 min, then returned back to 10% aqueous phase in 0.2 min, and re-equilibrated at 10% aqueous phase for 0.8 min. The flow rate was 300 µL/min and the injection volume was 5 µL. Mass spectrometry (MS) analyses were performed on a Sciex® API 4000 triple quadruple mass spectrometer equipped with a TurboIonSpray® interface in the positive ESI mode (Applied Biosystems MDS, San Francisco, CA). The multiple reaction monitoring (MRM) transitions and instrument settings were optimized for each compound. Equipment operation, data acquisition, and data integration were performed using Analyst version 1.4.2. software (Applied Biosystems, Foster City, CA).

Calculation. Apparent permeability coefficients (P_{app}) were calculated using the following equation:

$$P_{app} = \frac{V_R}{(A \times C_0)} \times \frac{dC}{dt}$$

where V_R is the volume in the receiver chamber (mL), A is the filter surface area (1.12 cm^2), C_0 is the initial concentration (µM) in the donor chamber, and dC/dt is the maximum (or initial) slope of the concentration (µM) vs. time (second) curve. The slope was calculated from the interval yielding the most linear rate of transfer spanning at least 2 sampling intervals.

Kinetic analysis of rosuvastatin was performed using GraphPad Prism® 5.02 for Windows (San Diego, CA). The active portion of B-to-A rosuvastatin transport across Caco-2 cell monolayers was isolated by subtracting the rate at 4°C from the corresponding rate at 37°C, and then the differential transport rates were fit to the Michaelis-Menten equation:

$$V = \frac{V_{\max} \cdot C}{K_m + C}$$

where V is the B-to-A rosuvastatin flux (pmol/cm^2/s) at a given concentration, C, of rosuvastatin, V_{max} is the maximal B-to-A flux, and K_m is the concentration of rosuvastatin at one-half of the

DMD Fast Forward. Published on March 29, 2011 as DOI: 10.1124/dmd.111.038075
This article has not been copyedited and formatted. The final version may differ from this version.

maximal B-to-A rate.

Statistical analysis. The significance of differences among multiple groups was determined by one-way ANOVA followed by post hoc Tukey tests. Differences were considered statistically significant when $p < 0.05$.

DMD Fast Forward. Published on March 29, 2011 as DOI: 10.1124/dmd.111.038075
This article has not been copyedited and formatted. The final version may differ from this version.

Results

Suppression of Efflux Transporters by shRNA in Caco-2 Cells. Following suppression of the expression of the major efflux transporters (P-gp, BCRP, and MRP2) in Caco-2 cells, by means of transduction with lentivirus vectors containing shRNA targeting transporter mRNAs, the transduced cells with the highest transporter suppression were selected. To determine potential off-target effects of the transduction process on these transporters we transduced Caco-2 cells with a viral vector containing shRNA that does not match any known human genes using the same transduction procedure. The suppression efficiency and selectivity were examined by measuring the mRNA expression of these efflux transporters using qPCR (Table 1). In VC cells the expression of P-gp, BCRP, and MRP2 mRNA was between 70% and 100% of the levels seen in un-transduced Caco-2 cells. In the KD cells, expression of targeted transporter genes was suppressed to 20% or less of the VC, whereas expression of non-targeted transporter genes remained 60%-100% of the VC. The suppression of efflux transporter protein expression by transduction with the shRNA-containing lentivirus was confirmed by Western blot analysis (Fig. 1). The transporter shRNA lentivirus-transduced cells (Lane B to D) produced much less corresponding transporter proteins than the VC-transduced cells (Lane A). Function of efflux transporters in the KD cells was assessed using prototypical substrates (Table 2). The efflux ratio of the P-gp substrate digoxin was 17.7 in VC cells and decreased to 7.4 (42% of VC) in P-gp KD cells without showing an appreciable change in BCRP KD and MRP2 KD cells. The BCRP substrate, E3S, exhibited a high efflux ratio (i.e., 48.5) in the VC cells, which was reduced to 10.2 (21% of VC cells) in the BCRP KD cells but remained roughly unchanged in P-gp KD and MRP2 KD cells. The efflux ratio of BSP, a MRP2 substrate, was reduced from 48.3 in VC cells to 2.6 in MRP2 KD cells.

Transport of Statin Drugs in Transporter KD Caco-2 Cells. Atorvastatin, fluvastatin, and rosuvastatin are commercially available in the acid form whereas lovastatin and simvastatin

DMD Fast Forward. Published on March 29, 2011 as DOI: 10.1124/dmd.111.038075
This article has not been copyedited and formatted. The final version may differ from this version.

are as lactones. Samples were analyzed by LC-MS/MS for both the acid and lactone forms of each compound. Following dosing, the statin acid drugs remained as acid form, with little conversion to the lactone form. On the other hand, the two lactone drugs showed substantial conversion to acid form during the course of the experiments. Atorvastatin acid was highly effluxed across the monolayers of VC cells. Its efflux was significantly diminished across monolayers of P-gp KD cells, and less so across monolayers of BCRP and MRP2 KD cells (Fig. 2A). The results indicate that P-gp was the major efflux transporter responsible for atorvastatin-acid efflux in this cell model, along with some contribution from both BCRP and MRP2. The decrease in atorvastatin acid efflux across transporter KD cell monolayers was mostly due to a decrease in the B-to-A transport as there was little change in the A-to-B transport compared to VC cell monolayers. Fluvastatin acid showed a similar pattern of permeability differences among the different cell lines (Fig. 2B). It was most highly effluxed across VC cell monolayers followed by across MRP2, BCRP and P-gp KD cell monolayers. Fluvastatin acid, similarly to the other statin acids, appears to be primarily effluxed by P-gp, with BCRP and MRP2 playing minor roles in the efflux of fluvastatin acid. The decreased efflux across monolayers of P-gp KD cells was associated with a significant decrease in the B-to-A permeability, similar to the observations obtained with atorvastatin. Rosuvastatin acid was also highly effluxed in VC cells (Fig. 2C). The B-to-A permeability coefficients and the efflux ratios for rosuvastatin acid are diminished in all three KD cell lines, compared to those in the VC cells, suggesting all three of the targeted efflux transporters play a role in excreting rosuvastatin across the apical membrane of the intestinal cells.

After dosing the lactone form, more than half of lovastatin in the receiver compartments was converted to the acid, and the drug was not effluxed in any of the cell lines (Fig. 3). The results indicate that the efflux transporters play no significant role in lovastatin lactone transport. In the same experiment after lovastatin lactone dosing, formation of lovastatin acid was also

monitored, and the permeability coefficients of formed lovastatin acid were high and comparable in both A-to-B and B-to-A directions (Fig. 3B). This high permeability would likely overwhelm any contribution of efflux or uptake transporters to the absorption of lovastatin acid in this model. Similar to lovastatin lactone, simvastatin lactone showed approximately 50% acid conversion in the receiver compartment, and no apparent efflux in any of the cell clones (Fig. 4). Simvastatin acid showed high transport rates in both A-to-B and B-to-A directions across the monolayers of VC cells and there was no significant difference between the A-to-B and B-to-A permeability coefficients. The KD cells did not show significant changes in the transport rates of simvastatin acid. Based on these findings one can conclude that efflux transporters likely play a negligible role in limiting the absorption of highly permeable statin lactones, such as lovastatin or simvastatin.

Involvement of drug efflux transporters in the transport of statin acids was further assessed using chemical inhibitors in order to compare the results using transporter KD cell lines or chemical inhibitors to dissect absorption and excretion pathways. Rosuvastatin acid showed the highest efflux among the statin acids tested in the study; therefore, this drug was chosen for the inhibition experiments. Before inhibition experiments, the kinetics of rosuvastatin B-to-A transport across Caco-2 monolayers was determined as a function of rosuvastatin concentration from 2 to 200 μM at 37°C and 4°C. Rosuvastatin B-to-A transport across Caco-2 monolayers was saturable and temperature-dependent (Fig. 5). Fitting differential transport rates between 37°C and 4°C to the Michaelis-Menten equation gave an apparent K_m of 98 ± 33 μM and a V_{max} of 137 ± 21 pmol/cm^2/min. The concentration and temperature dependence confirmed the involvement of a carrier-mediated efflux system(s) in rosuvastatin transport across Caco-2 monolayers. Rosuvastatin B-to-A transport was inhibited by various compounds (Fig. 6). Cyclosporine A (CsA), a broad inhibitor of efflux transporters; FTC, a selective inhibitor of BCRP; GF120918 an inhibitor of both P-gp and BCRP; MK571, an inhibitor of MRPs,

DMD Fast Forward. Published on March 29, 2011 as DOI: 10.1124/dmd.111.038075
This article has not been copyedited and formatted. The final version may differ from this version.

including MRP2; and verapamil, a selective inhibitor of P-gp, all decrease rosuvastatin efflux to some extent, suggesting the involvement of multiple efflux transporters in the efflux of this compound.

DMD Fast Forward. Published on March 29, 2011 as DOI: 10.1124/dmd.111.038075
This article has not been copyedited and formatted. The final version may differ from this version.

Discussion

The ABC efflux transporters, P-gp, BCRP, and MRP2, located in the apical membrane of enterocytes and in the canalicular membrane of hepatocytes, play important roles in the absorption of xenobiotics and facilitate the hepatobiliary elimination of xenobiotics and/or their metabolites. In this study we used Caco-2 cells in which efflux transporters had been knocked down using shRNA (Zhang et al., 2009), to investigate the role of efflux transporters in statin transport. Given the gene sequence specificity of RNAi silencing (Montgomery and Fire, 1998), shRNA-induced transporter knockdown is expected to avoid the cross-inhibition associated with chemical inhibitors (Watanabe et al., 2005; Wang et al., 2008). Despite the original expectation that RNAi-mediated gene silencing was specific, subsequent studies found that RNAi-mediated silencing may be associated with down-regulation of non-target genes, so called 'off-target effects' (Jackson et al., 2003). Furthermore, in certain animal models silencing or down-regulation of a transporter gene may lead to compensatory up-regulation of other genes (Chen et al., 2005b). To determine the knockdown efficiency and nonspecific effects of RNAi silencing in the current study, we measured the expression levels of the efflux transporters at both the mRNA and protein levels by qPCR and Western blot analysis. Knockdown of the transporter of interest was confirmed by both qPCR (Table 1) and Western blot results (Fig. 1). The qPCR analyses further revealed that up-regulation of non-target efflux transporters was virtually absent; instead, a slight down-regulation of certain non-target transporters was observed. Because down-regulation of off-target mRNA transcripts can hardly be avoided by the in-silico design of siRNA sequences (Echeverri and Perrimon, 2006; Tschuch et al., 2008), additional methods were proposed to reduce the off-target effects. One approach is to use 'nonspecific' or 'scrambled' siRNAs which have no physiological target as negative controls (Echeverri and Perrimon, 2006). Another approach is to target a single mRNA of interest with a pool of several different endonuclease-prepared siRNA molecules (Kittler et al., 2005). Furthermore, the viral-

based shRNA approach using lenti- or retroviruses is another option for reducing off-target effects, because viral delivery can be nearly 100% efficient in almost all cell types and the level of stable shRNA expression is comparatively modest, which causes minimal off-target effects with sustained silencing of the target gene (Tschuch et al., 2008). Therefore, in this current study we employed lentivirus-based shRNA gene silencing to generate the transporter KD cell lines, and used the cells transduced with nonspecific shRNA vector as a negative control in the transport experiments.

The large decrease in B-to-A transport of atorvastatin in P-gp KD Caco-2 cells (Fig. 1A) indicates that P-gp is an important mediator of atorvastatin efflux, an observation consistent with the conclusions of two previous studies in Caco-2 cells (Wu et al., 2000; Hochman et al., 2004). The smaller reduction in BCRP and MRP2 KD Caco-2 cells suggests that these transporters play lesser roles in atorvastatin transport. In spite of *in vitro* evidence showing the interaction of atorvastatin with P-gp (Hochman et al., 2004; Chen et al., 2005a), the *in vivo* role of P-gp in statin drug interactions remains unclear (Holtzman et al., 2006). This is partly because atorvastatin is metabolized by CYP3A4, and drugs that interact with atorvastatin are frequently substrates/inhibitors of both P-gp and CYP3A4. Despite these limitations, numerous pharmacokinetic drug interactions associated with atorvastatin have been reported (Boyd et al., 2000; Mazzu et al., 2000; Asberg et al., 2001). The affinity of atorvastatin for all three intestinal luminal efflux transporters could hamper its intestinal permeation, which may explain its moderate (30%) absorption in humans despite its relatively high lipophilicity (Neuvonen et al., 2006).

The two other acid statins, fluvastatin acid and rosuvastatin acid, were found to be substrates for P-gp, BCRP, and MRP2 in the transporter KD Caco-2 cell system (Fig. 2, B and C). These results agree with a study in which MRPs were reported to mediate the efflux of fluvastatin in Caco-2 cells (Lindahl et al., 2004). As is the case with atorvastatin, fluvastatin and

rosuvastatin were identified as P-gp substrates *in vitro*, but evidence of their involvement in P-gp-mediated drug interactions *in vivo* is scarce. In fact, co-administration of these statins with the P-gp substrate digoxin did not cause clinically significant adverse reactions to either statin drugs or digoxin (Garnett et al., 1994; Martin et al., 2002). The apparent absence of P-gp-based drug interactions might be due to the involvement of multiple efflux transporters as for atorvastatin. The report that BCRP polymorphism alters the AUC and C_{max} but not the elimination half-life (t½) suggests that the effect of BCRP on fluvastatin and rosuvastatin pharmacokinetics occurs primarily in the intestinal mucosa during the absorption of the acid forms of the drugs (Zhang et al., 2006; Keskitalo et al., 2009a; Keskitalo et al., 2009b).

Another similarity shared by atorvastatin, fluvastatin and rosuvastatin, the three acid statins, is the little acid-to-lactone conversion during transport. In light of a study showing that following oral administration of atorvastatin acid to healthy volunteers, atorvastatin lactone was found in plasma (Kantola et al., 1998), our results suggest that acid statins exist predominately in the native acid form in the gastrointestinal tract, with their lactonization occuring post absorption, most likely in the liver through the CoASH-dependent and glucuronidation pathways (Prueksaritanont et al., 2002). In contrast to the acid statins, the lactone statins (lovastatin and simvastatin) showed substantial lactone-to-acid conversion during transport as nearly equal amounts of the lactone and acid forms appeared in the receiver chambers (Fig. 3 and Fig. 4). Hydrolysis of statin lactones to statin acids in Caco-2 assays appeared to involve both spontaneous chemical conversion and enzymatic processes. Since lipophilic compounds often can permeate cell membranes and show low efflux in cell monolayers, the relatively high lipophilicity of lovastatin and simvastatin (Neuvonen et al., 2006) suggests that efflux transporter activity is unlikely to be a significant barrier for these compounds, consistent with a suggestion made in a previous study (Polli et al., 2001). Our finding that lactone statins were either non-substrates or weak substrates for P-gp is in agreement with other *in vitro* studies (Hochman et

al., 2004; Chen et al., 2005a).

Lastly, we used rosuvastatin as a model compound to compare results from the transporter KD cells with results from chemical inhibitors in identifying the involvement of efflux transporters (Fig. 6). Inhibition of apical efflux transporters normally results in a decrease in B-to-A transport accompanied by an increase in A-to-B transport of a substrate (Polli et al., 2001). CsA, a broad inhibitor of ABC efflux transporters, partially inhibited the B-to-A transport of rosuvastatin in Caco-2 cells, indicating the involvement of these transporter(s). Inhibitions by FTC and GF120918 are consistent with rosuvastatin being a substrate of BCRP. A slight inhibition by verapamil suggests that P-gp plays only a minor role in rosuvastatin transport, an observation that contrasts with results from transporter KD cells and with findings from a previous study (Kitamura et al., 2008). The finding that the MRP inhibitor MK571 completely abolished rosuvastatin efflux was unexpected because it appears to suggest that rosuvastatin was solely transported by MRP2 in Caco-2 cells, a possibility that conflicts with evidence of BCRP involvement found in this and other studies (Zhang et al., 2006; Kitamura et al., 2008; Keskitalo et al., 2009b). An alternative explanation is that MK571 cross-inhibits other efflux transporters as reported previously (Wang et al., 2008). Together, these results highlight the difficulties associated with relying only on chemical inhibitors to identify drug transporter interactions.

In conclusion, the transporter KD Caco-2 system permitted to identify the involvement of efflux transporters in statin transport. The statins in active β-hydroxy acid form were transported to some extent by P-gp, BCRP, and MRP2 in Caco-2 cells. The relatively high permeability of the lactone statins makes it difficult to detect directional transport in monolayer transport experiments. Our results showed that lactone statins are significantly hydrolyzed to the acid form in Caco-2 and KD cells. *In vivo*, the cooperative roles of intestinal transporters (of the acid form) and hydrolysis of the lactone form influence the pharmacokinetics of statin drugs

(Keskitalo et al., 2008; Keskitalo et al., 2009a). The current study demonstrates that the transporter KD Caco-2 system is a straightforward approach to assess drug-transporter interactions. Its human origin makes results relevant to human studies and avoids the species differences in statin interactions with efflux transporters that have been observed (Kitamura et al., 2008). In addition, Caco-2 cells express a basolateral uptake system that is essential for statins to reach apical efflux transporters. Due to the absence of this basolateral uptake transporter in MDCK cells, statin efflux could not be detected in non- or single-transfected MDCK cells (Kitamura et al., 2008). Overall, the transporter KD Caco-2 cells provide a valuable tool to study drug interactions with human transporters *in vitro* (Watanabe et al., 2005).

DMD Fast Forward. Published on March 29, 2011 as DOI: 10.1124/dmd.111.038075
This article has not been copyedited and formatted. The final version may differ from this version.

Acknowledgements. The authors wish to thank Samantha Allen, Erica A. Weiskircher, James L. Merdink, Grainne McMahon Tobin and Yuehua Huang for expert technical assistance.

DMD Fast Forward. Published on March 29, 2011 as DOI: 10.1124/dmd.111.038075
This article has not been copyedited and formatted. The final version may differ from this version.

Authorship contributions

Participated in research design: Li, Hidalgo, Volpe, Owen, Bode, and Zhang

Conducted experiments: Volpe and Wang

Contributed new reagents or analytic tools: Not Applicable

Performed data analysis: Li and Volpe

Wrote or contributed to the writing of the manuscript: Li, Hidalgo, Volpe, and Owen

References

Asberg A, Hartmann A, Fjeldsa E, Bergan S and Holdaas H (2001) Bilateral pharmacokinetic interaction between cyclosporine A and atorvastatin in renal transplant recipients. *Am J Transplant* **1:**382-386.

Boyd RA, Stern RH, Stewart BH, Wu X, Reyner EL, Zegarac EA, Randinitis EJ and Whitfield L (2000) Atorvastatin coadministration may increase digoxin concentrations by inhibition of intestinal P-glycoprotein-mediated secretion. *J Clin Pharmacol* **40:**91-98.

Chen C, Lin J, Smolarek T and Tremaine L (2007) P-glycoprotein has differential effects on the disposition of statin acid and lactone forms in mdr1a/b knockout and wild-type mice. *Drug Metab Dispos* **35:**1725-1729.

Chen C, Mireles RJ, Campbell SD, Lin J, Mills JB, Xu JJ and Smolarek TA (2005a) Differential interaction of 3-hydroxy-3-methylglutaryl-coa reductase inhibitors with ABCB1, ABCC2, and OATP1B1. *Drug Metab Dispos* **33:**537-546.

Chen C, Slitt AL, Dieter MZ, Tanaka Y, Scheffer GL and Klaassen CD (2005b) Up-regulation of Mrp4 expression in kidney of Mrp2-deficient TR- rats. *Biochem Pharmacol* **70:**1088-1095.

Echeverri CJ and Perrimon N (2006) High-throughput RNAi screening in cultured cells: a user's guide. *Nat Rev Genet* **7:**373-384.

Elsby R, Surry DD, Smith VN and Gray AJ (2008) Validation and application of Caco-2 assays for the in vitro evaluation of development candidate drugs as substrates or inhibitors of P-glycoprotein to support regulatory submissions. *Xenobiotica* **38:**1140-1164.

Garnett WR, Venitz J, Wilkens RC and Dimenna G (1994) Pharmacokinetic effects of fluvastatin in patients chronically receiving digoxin. *Am J Med* **96:**84S-86S.

Hidalgo IJ (2001) Assessing the absorption of new pharmaceuticals. *Curr Top Med Chem* **1:**385-401.

Hochman JH, Pudvah N, Qiu J, Yamazaki M, Tang C, Lin JH and Prueksaritanont T (2004) Interactions of human P-glycoprotein with simvastatin, simvastatin acid, and atorvastatin. *Pharm Res* **21:**1686-1691.

Holtzman CW, Wiggins BS and Spinler SA (2006) Role of P-glycoprotein in statin drug interactions. *Pharmacotherapy* **26:**1601-1607.

Huang L, Wang Y and Grimm S (2006) ATP-dependent transport of rosuvastatin in membrane vesicles expressing breast cancer resistance protein. *Drug Metab Dispos* **34:**738-742.

Ieiri I, Higuchi S and Sugiyama Y (2009) Genetic polymorphisms of uptake (OATP1B1, 1B3) and efflux (MRP2, BCRP) transporters: implications for inter-individual differences in the pharmacokinetics and pharmacodynamics of statins and other clinically relevant drugs. *Expert Opin Drug Metab Toxicol* **5:**703-729.

Jackson AL, Bartz SR, Schelter J, Kobayashi SV, Burchard J, Mao M, Li B, Cavet G and Linsley PS (2003) Expression profiling reveals off-target gene regulation by RNAi. *Nat Biotechnol* **21:**635-637.

Kantola T, Kivisto KT and Neuvonen PJ (1998) Effect of itraconazole on the pharmacokinetics of atorvastatin. *Clin Pharmacol Ther* **64:**58-65.

Keskitalo JE, Kurkinen KJ, Neuvoneni PJ and Niemi M (2008) ABCB1 haplotypes differentially affect the pharmacokinetics of the acid and lactone forms of simvastatin and atorvastatin. *Clin Pharmacol Ther* **84:**457-461.

Keskitalo JE, Pasanen MK, Neuvonen PJ and Niemi M (2009a) Different effects of the ABCG2 c.421C>A SNP on the pharmacokinetics of fluvastatin, pravastatin and simvastatin. *Pharmacogenomics* **10:**1617-1624.

Keskitalo JE, Zolk O, Fromm MF, Kurkinen KJ, Neuvonen PJ and Niemi M (2009b) ABCG2 polymorphism markedly affects the pharmacokinetics of atorvastatin and rosuvastatin. *Clin Pharmacol Ther* **86:**197-203.

Kitamura S, Maeda K, Wang Y and Sugiyama Y (2008) Involvement of multiple transporters in the hepatobiliary transport of rosuvastatin. *Drug Metab Dispos* **36:**2014-2023.

Kittler R, Heninger AK, Franke K, Habermann B and Buchholz F (2005) Production of endoribonuclease-prepared short interfering RNAs for gene silencing in mammalian cells. *Nat Methods* **2:**779-784.

Lindahl A, Sjoberg A, Bredberg U, Toreson H, Ungell AL and Lennernas H (2004) Regional intestinal absorption and biliary excretion of fluvastatin in the rat: possible involvement of mrp2. *Mol Pharm* **1:**347-356.

Martin PD, Kemp J, Dane AL, Warwick MJ and Schneck DW (2002) No effect of rosuvastatin on the pharmacokinetics of digoxin in healthy volunteers. *J Clin Pharmacol* **42:**1352-1357.

Mazzu AL, Lasseter KC, Shamblen EC, Agarwal V, Lettieri J and Sundaresen P (2000) Itraconazole alters the pharmacokinetics of atorvastatin to a greater extent than either cerivastatin or pravastatin. *Clin Pharmacol Ther* **68:**391-400.

Montgomery MK and Fire A (1998) Double-stranded RNA as a mediator in sequence-specific genetic silencing and co-suppression. *Trends Genet* **14:**255-258.

Neuvonen PJ, Niemi M and Backman JT (2006) Drug interactions with lipid-lowering drugs: mechanisms and clinical relevance. *Clin Pharmacol Ther* **80:**565-581.

Polli JW, Wring SA, Humphreys JE, Huang L, Morgan JB, Webster LO and Serabjit-Singh CS (2001) Rational use of in vitro P-glycoprotein assays in drug discovery. *J Pharmacol Exp Ther* **299:**620-628.

Prueksaritanont T, Subramanian R, Fang X, Ma B, Qiu Y, Lin JH, Pearson PG and Baillie TA (2002) Glucuronidation of statins in animals and humans: a novel mechanism of statin lactonization. *Drug Metab Dispos* **30:**505-512.

Tschuch C, Schulz A, Pscherer A, Werft W, Benner A, Hotz-Wagenblatt A, Barrionuevo LS, Lichter P and Mertens D (2008) Off-target effects of siRNA specific for GFP. *BMC Mol Biol* **9:**60.

Wang Q, Strab R, Kardos P, Ferguson C, Li J, Owen A and Hidalgo IJ (2008) Application and limitation of inhibitors in drug-transporter interactions studies. *Int J Pharm* **356:**12-18.

Watanabe T, Onuki R, Yamashita S, Taira K and Sugiyama Y (2005) Construction of a functional transporter analysis system using MDR1 knockdown Caco-2 cells. *Pharm Res* **22:**1287-1293.

Wu X, Whitfield LR and Stewart BH (2000) Atorvastatin transport in the Caco-2 cell model: contributions of P-glycoprotein and the proton-monocarboxylic acid co-transporter. *Pharm Res* **17:**209-215.

Zhang W, Li J, Allen SM, Weiskircher EA, Huang Y, George RA, Fong RG, Owen A and Hidalgo IJ (2009) Silencing the breast cancer resistance protein expression and function in caco-2 cells using lentiviral vector-based short hairpin RNA. *Drug Metab Dispos* **37:**737-744.

Zhang W, Yu BN, He YJ, Fan L, Li Q, Liu ZQ, Wang A, Liu YL, Tan ZR, Fen J, Huang YF and Zhou HH (2006) Role of BCRP 421C>A polymorphism on rosuvastatin pharmacokinetics in healthy Chinese males. *Clin Chim Acta* **373:**99-103.

Footnotes

†This study was supported in part by a research grant [1R43FD003482-01] from The Food and Drug Administration.

*Disclaimer: The findings and conclusions in this article have not been formally disseminated by the Food and Drug Administration and should not be construed to represent any Agency determination or policy.

DMD Fast Forward. Published on March 29, 2011 as DOI: 10.1124/dmd.111.038075
This article has not been copyedited and formatted. The final version may differ from this version.

Legends for figures

FIG.1. Expression of P-gp, BCRP and MRP2 proteins in VC and transporter KD cells. Forty-five micrograms of protein was loaded for Western blot assay. Lane A, non-specific shRNA VC-transduced cells; lane B, shRNA/Pgp knockdown cells; lane C, shRNA/BCRP knockdown cells; lane D, shRNA/MRP2 knockdown cells.

FIG. 2. Bidirectional transport of acid statins across the monolayers of transporter KD cells. Statin drug was dosed in the acid form, both acid and lactone forms were monitored, the concentration of the lactone form was negligible (data not shown): atorvastatin acid (A), fluvastatin acid (B), rosuvastatin acid (C). Each bar represents the mean ± S.D.; n = 3. *, $p < 0.05$; **, $p < 0.01$; ***, $p < 0.001$ significance level of the difference from the corresponding rates in the VC cells.

FIG. 3. Bidirectional transport of lovastatin lactone across monolayers of VC and transporter KD cells. Statin drug was dosed in lactone form: lovastatin lactone (A), lovastatin acid (B), sum of lovastatin acid and lactone (C). Each bar represents the mean ± S.D.; n = 3.

Fig. 4. Bidirectional transport of simvastatin lactone across monolayers of VC and transporter KD cells. Statin drug was dosed in lactone form: simvastatin lactone (A), simvastatin acid (B), sum of simvastatin acid and lactone (C). Each bar represents the mean ± S.D.; n = 3.

FIG. 5. Secretory transport kinetics of rosuvastatin across Caco-2 cells. The B-to-A transport of rosuvastatin was determined as a function of rosuvastatin concentration. Solid circles represent the transport rates at 37°C and open circles represent the rates at 4°C. Each point represents the mean ± S.D.; n = 3; the error bars are smaller than the symbols at 4°C. The solid line

represents the best fit of differential rates between 37°C and 4°C to the Michaelis-Menten equation.

FIG. 6. Effects of chemical inhibitors on rosuvastatin transport in Caco-2 cells. Caco-2 cell monolayers were pre-incubated 30-min with efflux transporter inhibitors: 10 μM cyclosporine A (CsA), 10 μM fumitremorgin C (FTC), 5 μM GF120918, 30 μM MK571, or 100 μM verapamil, then bidirectional transport experiments of 10 μM rosuvastatin were conducted in the absence or presence of the inhibitors. Each bar represents the mean ± S.D.; n = 3. *, $p < 0.05$; **, $p < 0.01$; ***, $p < 0.001$ significance level of the difference from the corresponding rates in the untreated Caco-2 cells.

DMD Fast Forward. Published on March 29, 2011 as DOI: 10.1124/dmd.111.038075
This article has not been copyedited and formatted. The final version may differ from this version.

TABLE 1

Expression level of efflux transporter mRNAs in shRNA induced knockdown cells; the level in un-transduced parental Caco-2 cells was set to 1.0 as reference

mRNA	VC	P-gp KD	BCRP KD	MRP2 KD
P-gp	0.71 ± 0.34	0.20 ± 0.11	0.78 ± 0.33	0.88 ± 0.17
BCRP	0.71 ± 0.03	0.62 ± 0.15	0.14 ± 0.04	1.08 ± 0.15
MRP2	1.00 ± 0.09	1.00 ± 0.09	0.63 ± 0.25	0.14 ± 0.03

Data are means ± S.D., n = 3.

DMD Fast Forward. Published on March 29, 2011 as DOI: 10.1124/dmd.111.038075
This article has not been copyedited and formatted. The final version may differ from this version.
DMD #38075

TABLE 2

Functional activity of efflux transporters in knockdown cells

Substrate/ Transporter	Cell clone	$P_{app\ A\rightarrow B}$*	$P_{app\ B\rightarrow A}$*	Efflux ratio	% of VC
Digoxin/ P-gp	VC	1.14 ± 0.07	20.09 ± 1.36	17.7	--
	P-gp KD	1.59 ± 0.10	11.78 ± 1.22	7.4	42%
	BCRP KD	0.54 ± 0.04	9.46 ± 1.60	17.7	100%
	MRP2 KD	0.89 ± 0.20	19.00 ± 0.29	21.4	121%
E3S/ BCRP	VC	0.57 ± 0.02	27.17 ± 1.08	48.5	--
	P-gp KD	0.52 ± 0.04	22.90 ± 2.98	43.6	90%
	BCRP KD	1.03 ± 0.02	10.50 ± 2.81	10.2	21%
	MRP2 KD	0.54 ± 0.04	33.46 ± 1.09	62.2	128%
BSP/ MRP2	VC	0.03 ± 0.05	1.45 ± 0.27	48.3	--
	MRP2 KD	0.34 ± 0.12	0.90 ± 0.14	2.6	5%

*P_{app} values are expressed as the means ± S.D. ($x10^{-6}$, cm/s), n = 3.

DMD Fast Forward. Published on March 29, 2011 as DOI: 10.1124/dmd.111.038075
This article has not been copyedited and formatted. The final version may differ from this version.

FIG 1

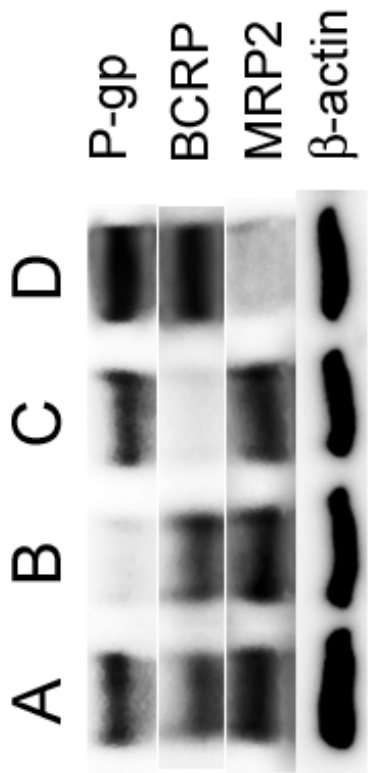

DMD Fast Forward. Published on March 29, 2011 as DOI: 10.1124/dmd.111.038075
This article has not been copyedited and formatted. The final version may differ from this version.

FIG 2

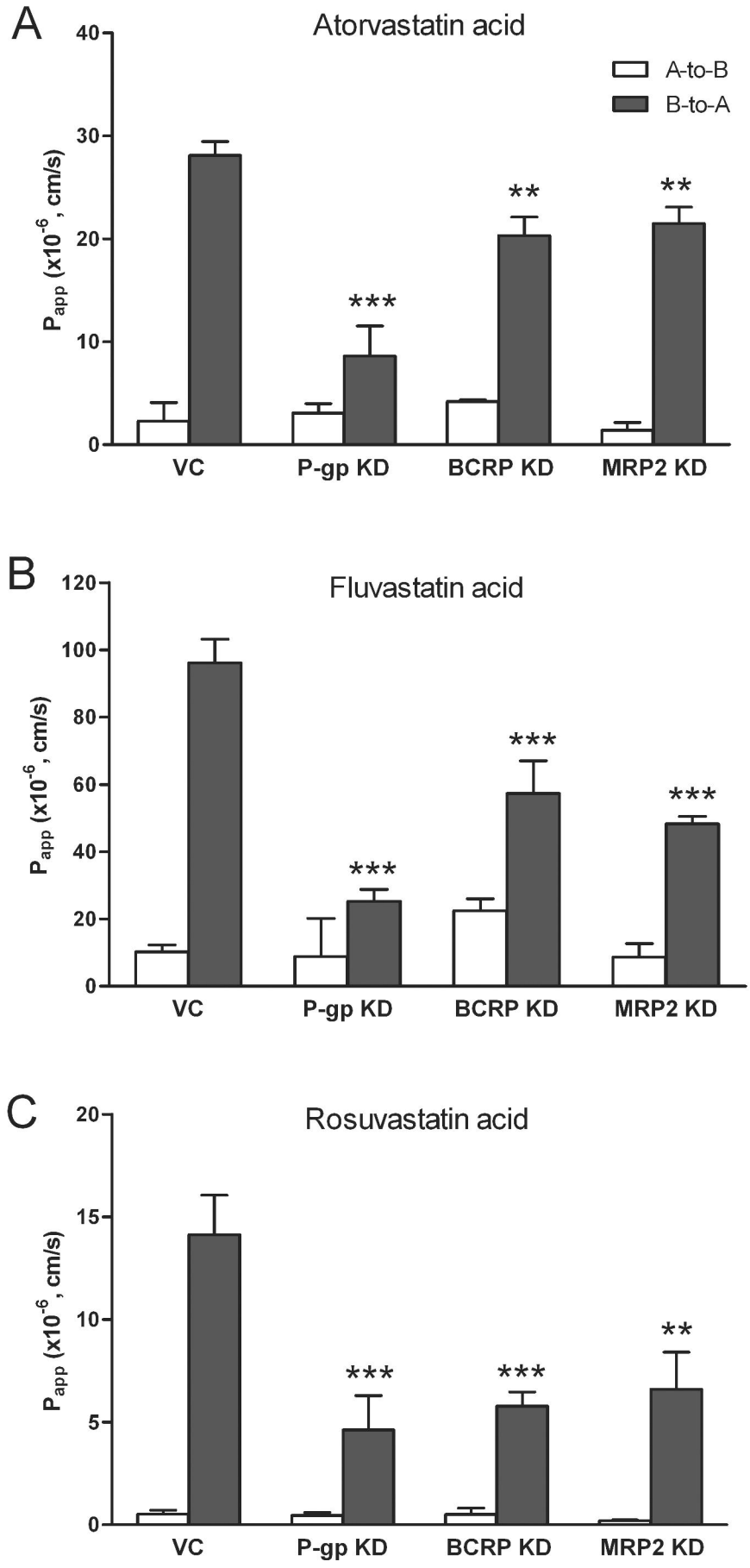

DMD Fast Forward. Published on March 29, 2011 as DOI: 10.1124/dmd.111.038075
This article has not been copyedited and formatted. The final version may differ from this version.

FIG 3

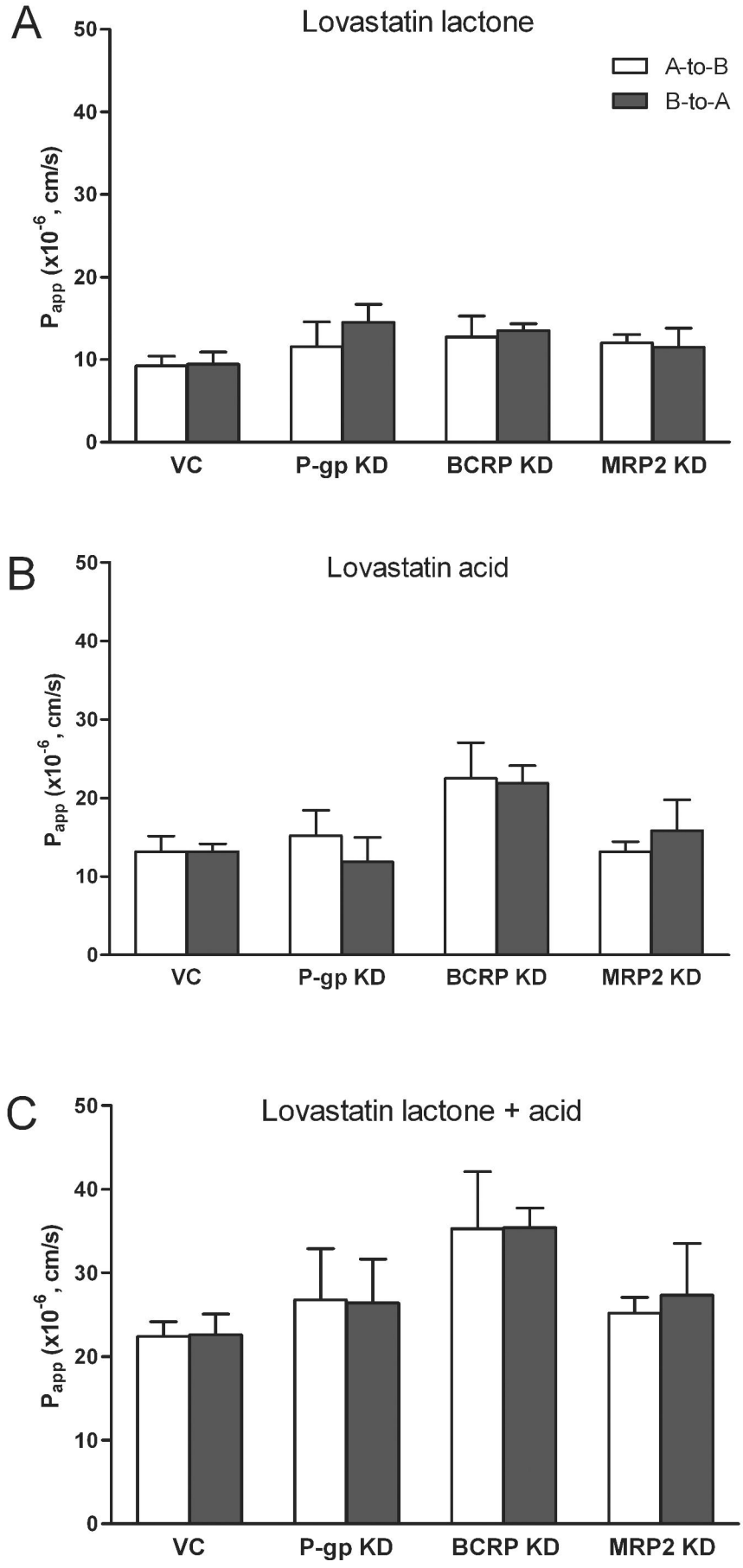

DMD Fast Forward. Published on March 29, 2011 as DOI: 10.1124/dmd.111.038075
This article has not been copyedited and formatted. The final version may differ from this version.

FIG 4

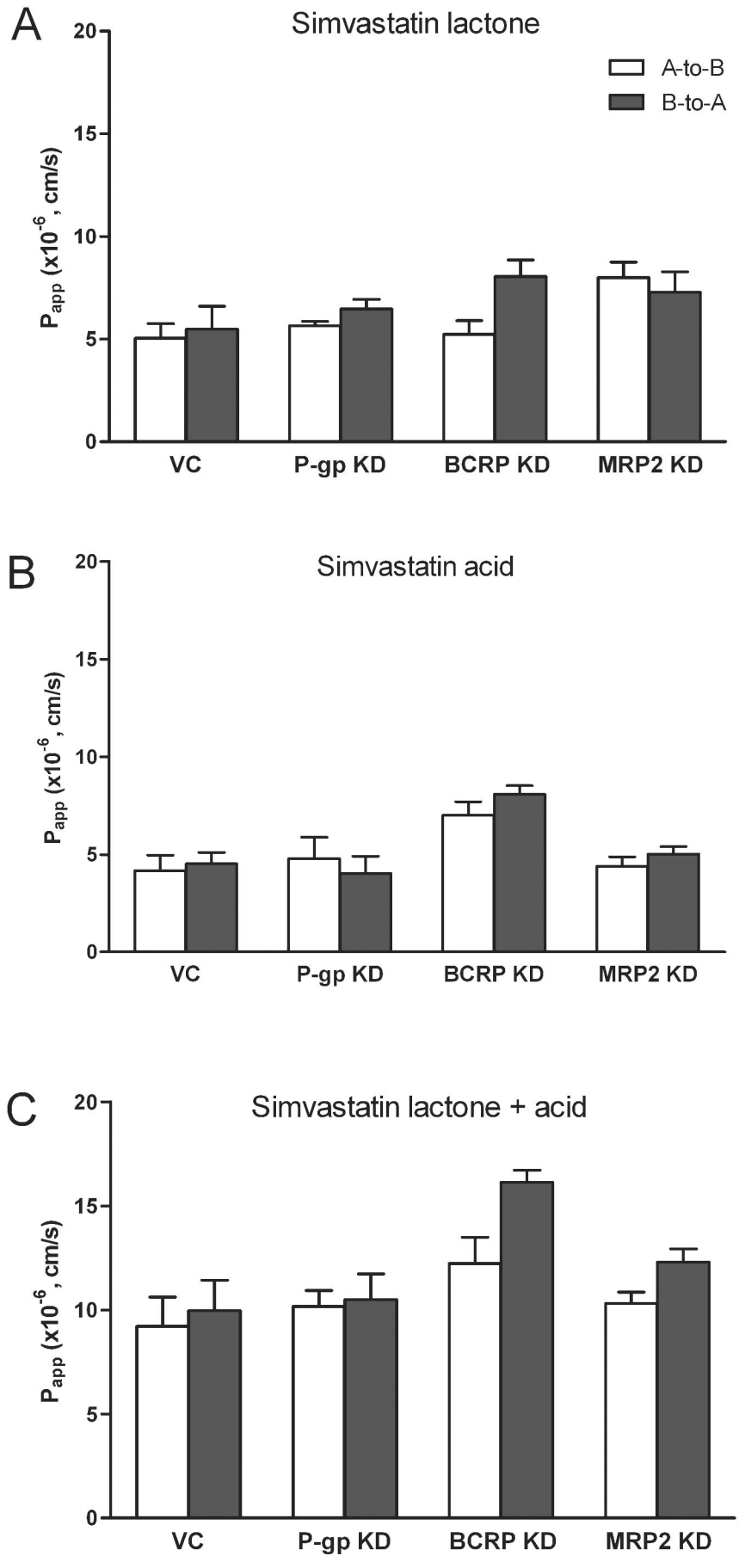

DMD Fast Forward. Published on March 29, 2011 as DOI: 10.1124/dmd.111.038075
This article has not been copyedited and formatted. The final version may differ from this version.

FIG 5

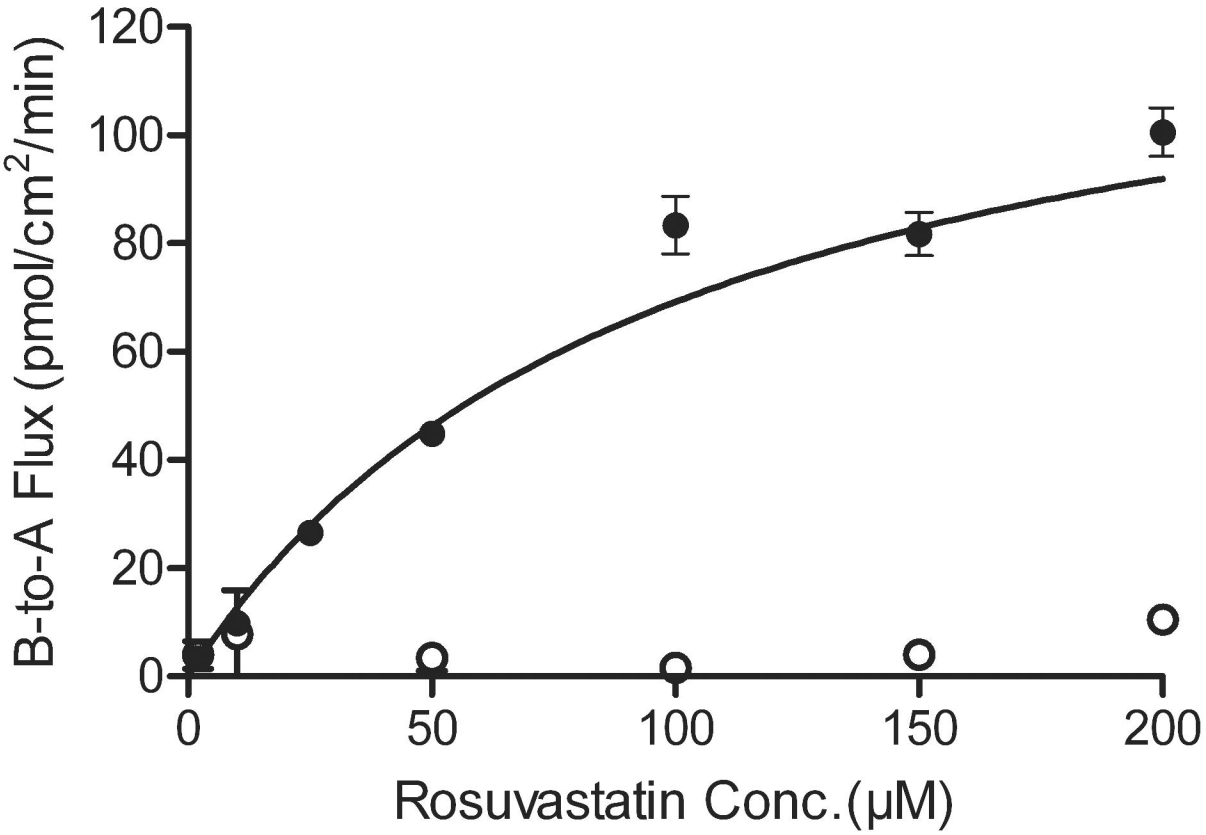

DMD Fast Forward. Published on March 29, 2011 as DOI: 10.1124/dmd.111.038075
This article has not been copyedited and formatted. The final version may differ from this version.

FIG 6